

ARTICLE

Open Access

Annonacin promotes selective cancer cell death via NKA-dependent and SERCA-dependent pathways

Andreas Yiallouris^{1,2}, Ioannis Patrikios¹, Elizabeth O. Johnson^{1,2}, Evangelia Sereti³, Konstantinos Dimas⁴, Cristian De Ford⁴, Natalia U. Fedosova⁵, Wolfgang F. Graier⁶, Kleitos Sokratous⁷, Kyriakos Kyriakou⁷ and Anastasis Stephanou¹

Abstract

In the healthcare sector, phytochemicals are known to be beneficial by contributing or alleviating a variety of diseases. Studies have demonstrated the progressive effects of phytochemicals on immune-related diseases and to exhibit anticancer effects. *Graviola* tree is an evergreen tree with its extract (leaves and seeds) been reported having anticancer properties, but the precise target of action is not clear. Using an *in silico* approach, we predicted that annonacin, an *Acetogenin*, the active agent found in *Graviola* leaf extract (GLE) to potentially act as a novel inhibitor of both sodium/potassium (NKA) and sarcoplasmic reticulum (SERCA) ATPase pumps. We were able to validate and confirm the *in silico* studies by showing that GLE inhibited NKA and SERCA activity in intact cells. In the present study, we also demonstrated the antiproliferative and anticancer effects of GLE in a variety of cancer cell lines with limited toxic effects on non-transformed cells. Moreover, our results revealed that known inhibitors of both NKA and SERCA pumps could also promote cell death in several cancer cell lines. In addition, a mouse xenograft cancer model showed GLE as able to reduce tumor size and progression. Finally, bioprofiling studies indicated a strong correlation between overexpression of both NKA and SERCA gene expression vs. survival rates. Overall, our results demonstrated that GLE can promote selective cancer cell death via inhibiting NKA and SERCA, and thus can be considered as a potential novel treatment for cancer. After molecular analysis of GLE by liquid chromatography–mass spectrometry and ESI–QTOF–MS analysis, it was found that the MS spectrum of the high abundant chromatographic peak purified sample highly consisted of annonacin.

Introduction

Graviola, *Soursop*, *Cannonball*, *Brazilian Paw Paw*, and *Annona muricata* are names of an evergreen tree comprising 130 genera and 2300 species^{1,2} discovered in South and North America's rainforest³. The specific *Graviola* tree extracts from leaves and/or native population to treat various diseases and illnesses have used seeds. The molecules

extracted from *Graviola* tree leaves and/or seeds, known as *Acetogenins* are molecules with approximately 35–37 carbon atoms that have been described to be associated with anticancer properties against various cancer cell lines, including multidrug-resistant cancer cell lines^{4–6}. The exact cellular targets and the way of action of *Acetogenins* are still unclear. Recent studies show that annonacin, an *Acetogenin*, promotes cytotoxicity via a pathway inhibiting the mitochondrial complex I⁷. Others have reported that the anti-tumor activity of *Graviola* leaf extract (GLE) may be attributed to the downregulation of the epidermal growth factor receptor^{8–10}. GLE has also been reported to inhibit multiple metastatic and signaling pathways and to induce

Correspondence: Ioannis Patrikios (i.patrikios@euc.ac.cy) or Anastasis Stephanou (a.stephanou@euc.ac.cy)


¹School of Medicine, European University Cyprus, Nicosia, Cyprus

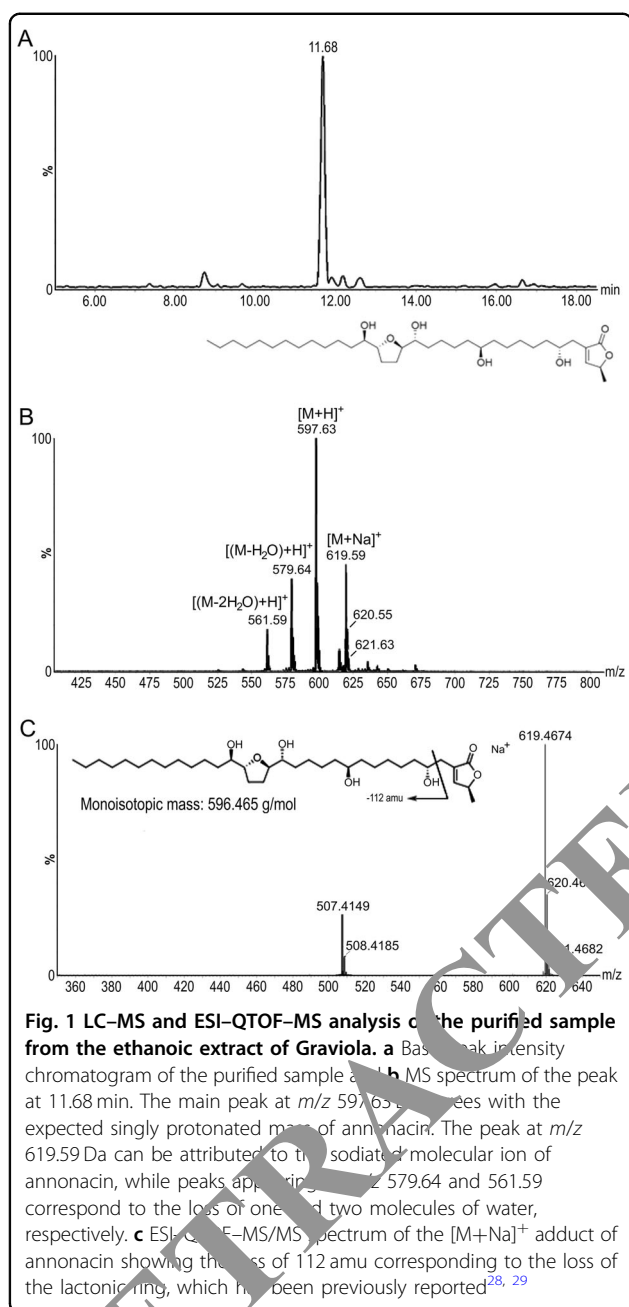
²School of Medicine, National and Kapodestrian University of Athens, Athens, Greece

Full list of author information is available at the end of the article.

Edited by G. Melino

© The Author(s) 2018

 **Open Access** This article is licensed under a Creative Commons Attribution 4.0 International License, which permits use, sharing, adaptation, distribution and reproduction in any medium or format, as long as you give appropriate credit to the original author(s) and the source, provide a link to the Creative Commons license, and indicate if changes were made. The images or other third party material in this article are included in the article's Creative Commons license, unless indicated otherwise in a credit line to the material. If material is not included in the article's Creative Commons license and your intended use is not permitted by statutory regulation or exceeds the permitted use, you will need to obtain permission directly from the copyright holder. To view a copy of this license, visit <http://creativecommons.org/licenses/by/4.0/>.



necrotic cell death by modulating the factors GLUT1, GLUT-1, LDHA, HKII, NF- κ B, and HIF-1 α ^{8–10}. Furthermore, GLE has been referred as a hypoxia-induced NADPH oxidase activity inhibitor on prostate cancer cells by reducing nuclear HIF-1 α levels, as well as it has been associated with inhibiting proliferative and clonogenic activities^{11–13}.

Although new chemotherapeutic drugs have improved the prognosis and outcome of a variety of human cancers, the major problem is that these types of therapies result in limited efficacy as well as cytotoxicity to the normal tissues and organs. Moreover, chemotherapeutic drugs also lead to drug-resistant and relapsed tumor growth.

Therefore, identification of drugs that are able to target the cancer cells without having toxic effects to normal cells would be more beneficial in the long term to the patients.

In the present study, an alcohol extract of the active ingredients found in GLE was investigated against various cancer cell lines for its antiproliferative and anticancer properties, as well as on non-cancer cell lines. *In silico* studies have identified a novel mode of action of the most abundant molecule found in GLE called annonacin that behaves as a potent inhibitor of the sarcoplasmic/endoplasmic reticulum (ER) calcium ATPase and sodium/potassium ATPase pumps. Overall, GLE is found to be associated with strong anticancer properties with limited toxicity.

Results

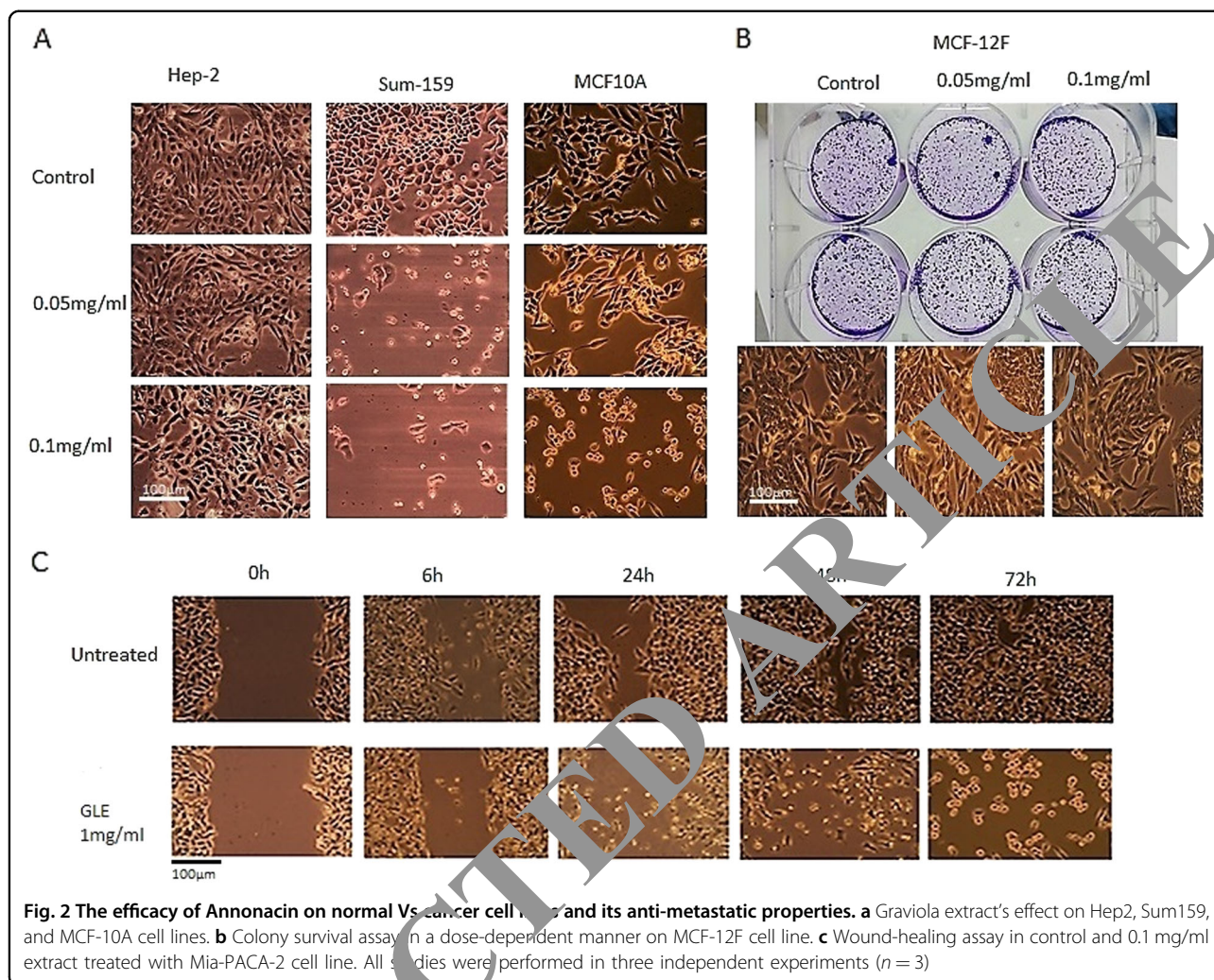
Thin-layer chromatography (TLC) and mass spectrometry

The TLC was used as one of the methods of isolating/purifying the annonacin ($R_f = 0.87$) molecule out of the ethanoic GLE pill extract (data not shown). Additionally, the ethanoic extract was further analyzed by LC-MS. The full MS spectrum of a chromatographic peak with a retention time (tR) of ~ 11.9 min showed a main singly charged ion peak at m/z 597.63 with additional peaks at m/z 619.59, 579.64, and 561.59 Da. The main peak was in good agreement with the expected protonated mass of annonacin. The additional peaks were attributed to sodium adduction (m/z 619.59) and to the loss of one and two water molecules (m/z 579.64 and 561.59 Da, respectively). The fraction eluted between 11.70 and 12.20 min was collected, reconstituted, redissolved, and subjected again to LC-MS analysis. The base peak intensity chromatogram of the purified sample is shown in Fig. 1a. The MS spectrum of the high abundant chromatographic peak at 11.68 min shows the same m/z peaks as described above (Fig. 1b), and therefore it can be concluded that the purified sample highly consisted of annonacin^{14,15}.

In addition, we further analyze the LC purified sample that was obtained from the ethanoic extract of Graviola, using high-resolution MS. Figure 1c shows the ESI-QTOF-MS/MS spectrum of the $[M+Na]^+$ adduct. The parent ion peak for the singly charged ion observed at m/z 619.4674 Da is in good agreement with the expected mass of annonacin (PubChem CID: 354398, monoisotopic mass: 596.465 g/mol) with a sodium adduct, which has also been reported previously^{1,2}. The daughter ion peak at m/z 507.4149 is generated from the loss of the lactonic ring.

In vitro cytotoxicity

In order to evaluate the antiproliferative and antitumor effects of the GLE pill ethanol extract, we treated different cancer cell lines. As indicated in Fig. 2a, the extract



induced cell death in a dose-dependent manner for Hep2 and Sum159. In contrast, the extract had limited death-inducing effects in a non-transformed cell line (MCF10A). Additionally, the non-toxic effects of the extract were also confirmed and observed using a clonogenic assay in non-transformed breast cell line (MCF12F) (Fig. 2b). Cell migration was also investigated using a monolayer wound-healing assay. As shown in Fig. 2c, cell movement was dramatically reduced in GLE-treated pancreatic cancer cells compared to untreated cells.

To quantify the antiproliferative effects of GLE, we performed the MTT (3-(4,5-dimethylthiazol-2-yl)-2,5-diphenyltetrazolium bromide) tetrazolium reduction assay. As indicated in Fig. 3a, GLE promoted cell death in a dose-dependent manner in MCF-7, Mia Paca-2, and SUM-159 cells ($IC_{50} = 0.01$ mg/ml). Once again, GLE had limited antiproliferative effects in normal non-transformed breast cell line (MCF-12F). In contrast, the chemotherapeutic drug cisplatin promoted cytotoxicity effects in all cancer cell lines as well as in the normal

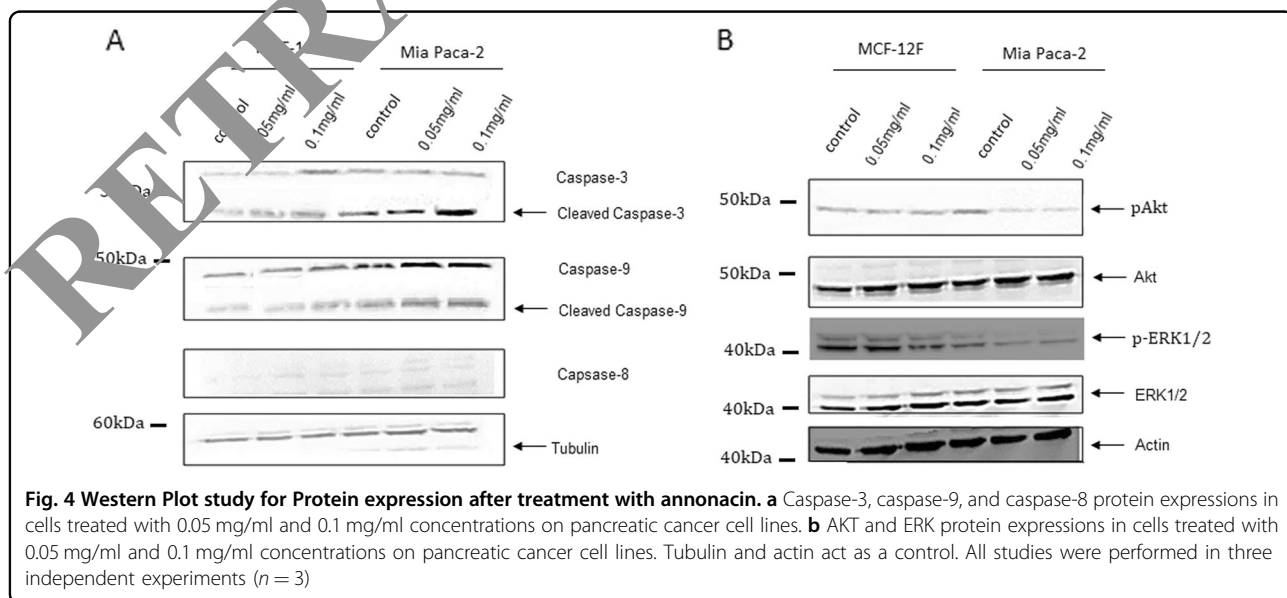
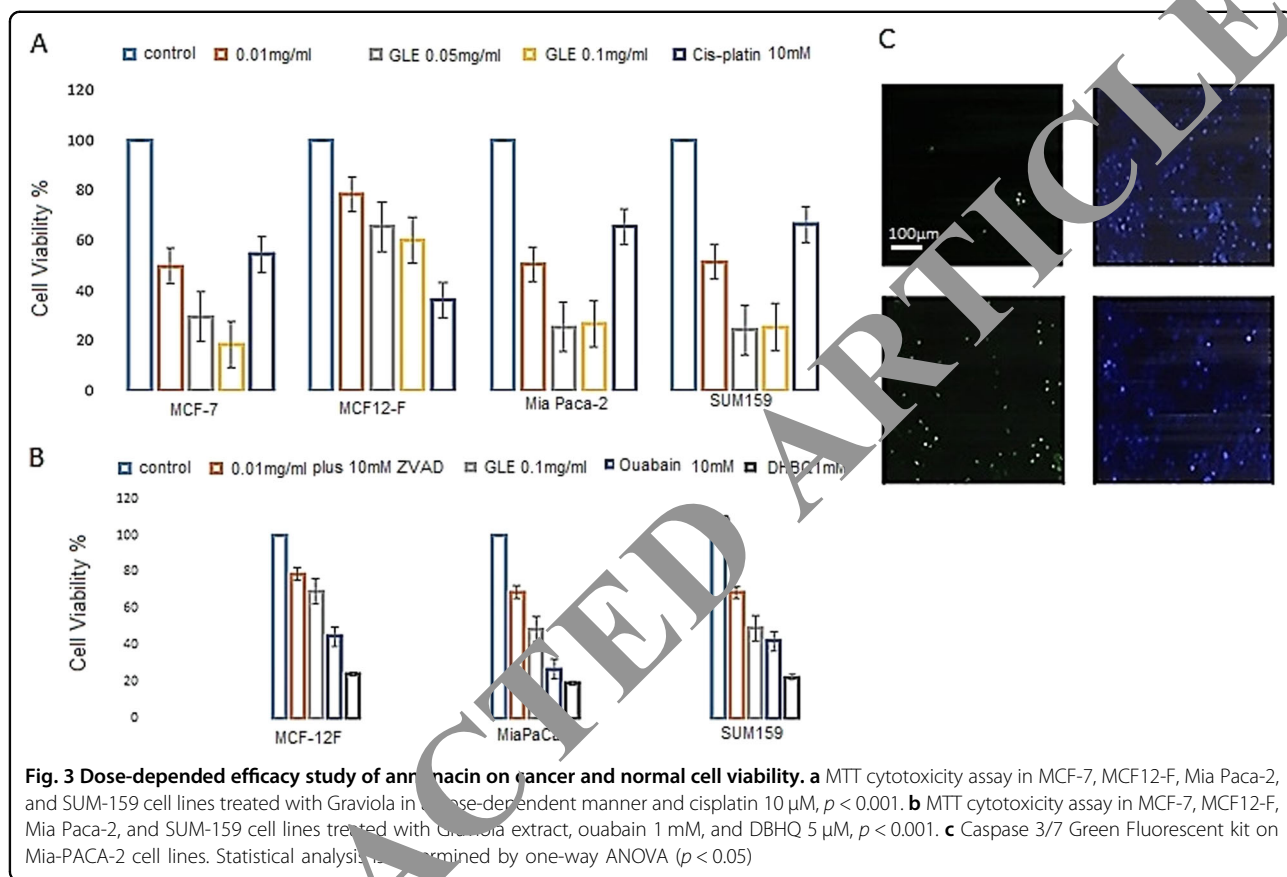
non-transformed cell line (Fig. 3a). These studies indicate that GLE is able to have selective antiproliferative and death-inducing effects in cancer cells with limited effects on normal cells. GLE had also been tested on human peripheral blood lymphocytes without any effects (data not shown).

To determine whether the cell death effects of GLE are mediated via a caspase-dependent pathway, we performed Caspase 3/7 green fluorescent assay. As shown in Fig. 3b, GLE promoted an apoptotic cell death pathway by inducing caspase 3 and 7, respectively, as indicated in its increase in fluorescent-staining activity (Fig. 3c). We also repeated our MTT assay in the presence and absence of Z-VAD-FMK, a cell-permeable pan-caspase inhibitor. Z-VAD-FMK was observed to partly reduce the antiproliferative effects of GLE (Fig. 3b), therefore suggesting that GLE death-inducing effects are partly mediated by an apoptotic pathway.

We additionally performed Western blotting to confirm whether GLE induced an apoptotic cell death

pathway. As shown in Fig. 4a, GLE induces both caspase 3 and caspase 9 expression in a dose-dependent manner in Mia Paca-2 cells, confirming our previous data above. GLE had limited effects on inducing caspase 3 and caspase 9 expression in normal MCF12F cell line (Fig. 4a). We also determine whether GLE is able to have effects on

both phospho-ERK and phospho-Akt that are well-known cell-proliferative markers. As indicated in Fig. 4a and b, GLE reduced both phospho-ERK and phospho-Akt in a dose-dependent manner in the Mia-PACA-2 cancer cells but had limited effects on normal MCF-12F cells.



In silico study of GLE and docking simulations corroborate the predicted targets of the structure similarity analysis

Due to the similarity of annonacin and the cardiotonic steroids (CSs) and given the fact that these compounds strongly inhibit NKA, docking experiments were performed with GOLD 5.2. The PDB 4HYT was chosen for the modeling studies since NKA was co-crystallized with ouabain in the high-affinity complex (E2P form). Before docking annonacin, a validation of the results was performed by re-docking ouabain and comparing to the crystal structure. Small deviations were obtained between the predicted and crystalized ouabain with a RMSD of 0.9591 Å, including the sugar moiety (Fig. 5a–c). Control docking experiments with the low-affinity complex of NKA and ouabain (PDB ID: 3A3Y) showed a considerable reduction in the docking¹⁶. The docking model showed that they also bind deep in the cavity (Fig. 5c). The crucial hydrogen bond with Thr797 was also predicted, as well as the van der Waals interactions with Phe783 in addition to hydrogen bonds with Asp121 and Asn122, thereby resembling the annonacin-binding mode as well. Notwithstanding, due to the high flexibility of these compounds, a conserved binding mode was not achieved among annonacin compounds but the main interactions were observed.

To further confirm the obtained results, a data pipeline was constructed in Knime[®] to compare the Tanimoto coefficients with the same database of cancer chemotherapeutics comprising 228 compounds. Annonacin showed similarities with both NKA and SERCA pump inhibitors (Table 1), meaning that they could be non-selective P-type ATPase inhibitors, such as ivermectin¹⁷, supporting the principal component analysis (PCA) results.

In order to validate our *in silico* data, we tested the effects of GLE on modulating both NKA and SERCA activity. As shown in Fig. 5, GLE inhibited NKA activity in a dose-dependent manner, where amygdalin, another nature extract, was used as a negative control. Furthermore, GLE strongly reduced SERCA activity (Fig. 5e). We also compared GLE against a known SERCA inhibitor 2,5-di-*t*-butyl-1,4-benzoquinone (BHQ), as indicated in Fig. 5f. These results demonstrated that GLE is a potent inhibitor of both NKA and SERCA pumps and confirms our *in silico* results.

As an additional piece of confirming information, we next examined whether known inhibitors of NKA and SERCA are able to promote cell death in cancer cell lines. As demonstrated in Fig. 5d, ouabain (a well-known NKA inhibitor) was shown to induce cell death in Mia-PACA-2 pancreatic cancer cells. Similar effects of ouabain-induced cell death were also observed in other cancer cells (data not shown). In addition, the SERCA inhibitor BHQ induced cell death in Mia-PACA-2 cells (Fig. 5d).

In vivo examination

Our results so far demonstrated that GLE may have a novel role in promoting cell death in cancer cells via inhibiting NKA-dependent and SERCA-dependent pathways. In order to show any association between NKA and SERCA expression and activity with cancer, we investigated a bioprofiling and prognostic value of NKA and SERCA in low vs. high-grade expression in various human cancers. As indicated in Fig. 6a and b, there was a clear and strong correlation between the high NKA isoform and SERCA isoform expression, and reduced survival rates in various cancers, including breast, colon, brain, and kidney cancers. These results indicated a strong association between the high expression of NKA and SERCA and survival rates. Finally, we also investigated the *in vivo* effects of GLE in xenograft cancer mouse model. GLE was tested for toxicity in NOD.CB17-Prkdcscid/J mice at doses as high as 400 mg/kg. Because of poor water solubility, a carrier based on DMSO and Cremophor ELP was selected for *in vivo* administrations. The extract was found to be toxic at doses higher than 50 mg/kg (400, 200, 100, 50, 25, and 10 mg/kg tested for toxicity) as mice died soon after the administration of these doses. At lower doses, i.e., 25 and 10 mg/kg, mice survived well. At these doses, mice showed no signs of toxicity or any other kind of side effects during the observation period of 2 weeks. Thus, we concluded that, under the experimental conditions used herein, the maximum tolerated dose (MTD) for the GLE is 25 mg/kg.

To further test *in vivo* efficacy, GLE was tested for activity against MIA PaCa-2 xenografts. The dose administered was the MTD (25 mg/kg) with mice receiving a total dose of 375 mg/kg during a period of 3 weeks. As it can be seen in Fig. 6c, the extract showed a trend to delay the growth of the tumors without reaching a statistical significance. Mice showed no signs of toxicity throughout the experimental period.

Discussion

P-type ATPases are ion pumps belonging to a superfamily of membrane proteins that catalyze the selective active transport of different ions across biological membranes of organelles or at the plasma membrane^{17,18}. Some of the most important and best-studied P-type ATPases are the NKA, SERCA pump, and the vacuolar H⁺-ATPases. Pharmacological inhibition of P-type ATPases has been proven successful for the treatment of some pathophysiological conditions, including cancer, and are thereby attractive drug targets^{18,19}.

In this study, further insights into the mechanism of cytotoxicity of GLE and its active ingredient annonacin were obtained. This study for the first time provides further insights into their mechanism of action by showing annonacin as a potent inhibitor of the NKA. The PCA

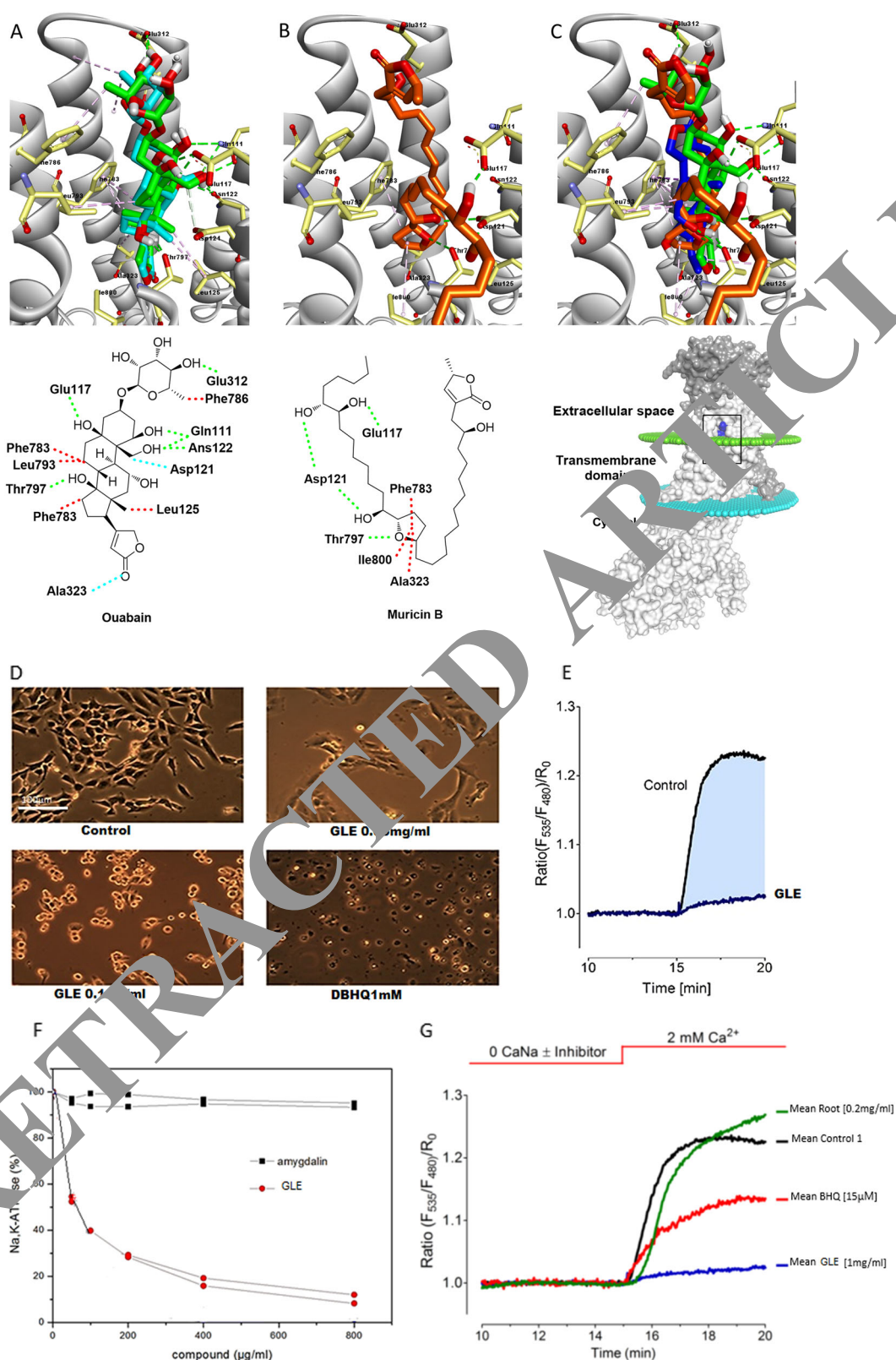


Fig. 5 Docking of muricins in the transmembrane domain of Na^+ and K^+ -ATPase (PDB ID: 4HYT) with GOLD 5.2. **a** Docking validation showing an overlay of co-crystallized (green) and docked ouabain (light blue). **b** *Annonacin*. **c** Overlay of the docked compounds. **d** Modulation of the ATPase activity of the Na^+ and K^+ -ATPase in vitro with extracts from *Annona muricata*. **e** Comparison of ER Ca^{2+} refilling kinetics under control conditions and in the presence of 1 mg/ml Graviola extract ($n = 5$). **f** Estimation of SERCA pump activity by measuring ER Ca^{2+} refilling of previously emptied ER ($n = 3-6$). **g** NKA pump inhibition curve showing the effect of Graviola (red) and amygdalin (black)

Table 1 Summary of in silico results from the PCA and docking studies

Compound	PC1	PC2	PC3	PC4	Target	Docking score ^b
Acetogenins	Very high	Non-aromatic	High	Very flexible	NKA SERCA	32.81 ± 3.97 ^c
Ouabain	High	Non-aromatic	Medium	Semi-rigid	NKA	45.31 ± 0.39
Ivermectin	Very high	Non-aromatic	High	Very flexible	NKA and SERCA ^a	29.59 ± 1.51 and 29.84 ± 0.86

PC1 characterizes the size, shape, and polarizability; PC2 indicates aromaticity and conjugation; PC3 describes lipophilicity, polarity, and H-bond capacity, and PC4 describes flexibility and rigidity. NKA Na⁺,K⁺-ATPase, SERCA Ca²⁺-ATPase, n.d. not determined

^aAccording to ChemGPS-NP, CheS-Mapper, and Knime[®]

^bObtained with GOLD 5.2 using PDBs 4HYT (NKA) and 2AGV (SERCA), data represent mean ± SD

^cMean docking scores of the compounds that belong to this class

analysis showed that they were placed in-between the alkylating agents (AA) and CSs, thus confirming the previously reported and the new target found herein. On the other hand, the natural products from the *Annonaceae* family of plants (*Annonaceous acetogenins*) are potent inhibitors of the NADH-ubiquinone reductase (complex I) activity of mammalian mitochondria²⁰. Nevertheless, our results additionally showed that they resemble ivermectin that prevents the ion transport of NKA (Table 1).

Biochemical analysis showed GLE, a major constituent annonacin as a direct inhibitor of NKA. Nevertheless, in the present study, the reported effect of partial charge distribution, and hence the long-range electrostatic interactions with Mg²⁺ observed with the carbonyl group of the lactone present in ouabain and site II²⁰ may be absent in the annonacin molecule presented herein. This is due to the predicted positioning of this moiety in the binding site (facing the extracellular phase of NKA), which may account for the strong decrease in the inhibitory activity compared to CSs, as shown in the biochemical experiments. CSs inhibit NKA in a low nanomolar range. Thus, an inverted positioning of the lactone moiety of annonacin in the binding site (lactone facing sites I and II) would prevent the pivotal hydrogen bond with Thr 797, explaining the predicted binding mode. Structural analysis of amino acid residues in the transmembrane helices M5–M6 of NKA has identified Phe783 and Thr797 as determinant residues for ouabain sensitivity; therefore, interactions with them play key roles in the inhibition of this ion pump,^{20,21} as also predicted for annonacin in the docking experiments (Figs 1a–c).

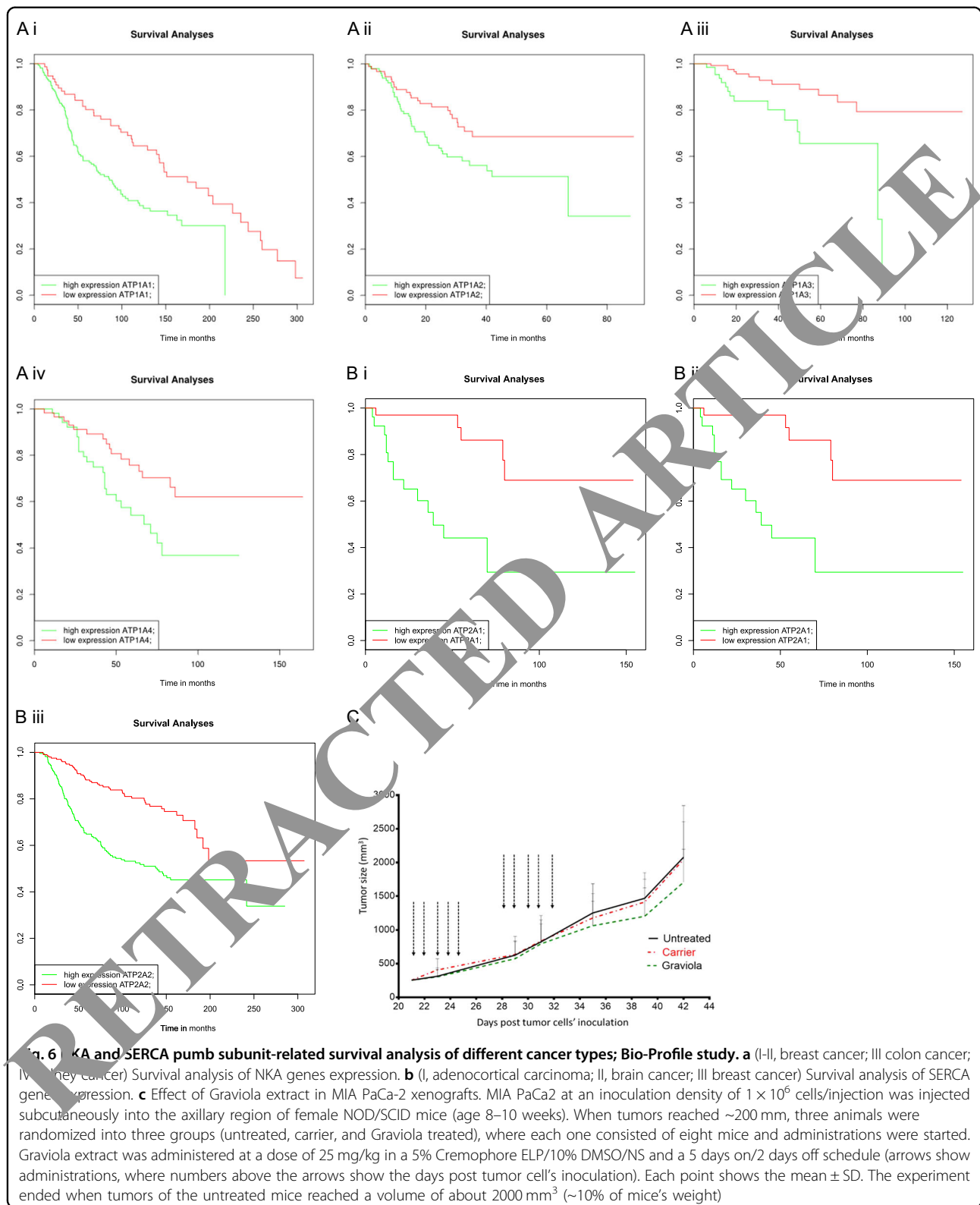
Altogether, our in silico study approaches along with our biochemical studies demonstrated a novel mechanism of action of annonacin explaining their known cytotoxic effects.

The ER and calcium signaling contribute to the regulation of normal and pathological signaling that is controlled by a family of protein channel enzymes that include the sarco/endoplasmic reticulum calcium ATPase pumps (SERCA)s²². There are 14 different

SERCA isoforms that are encoded by three ATP2A1–3 genes. A number of studies have reported that altered expressions of SERCA isoforms are associated with cancers. Similarly, sodium/potassium ATPase pumps (NKA) that regulate the levels of sodium and potassium within cells also play a role in signaling and their activity is also altered in several pathological disorders including cancer²³.

In the present study, we provide further insights into the antiproliferative and anticancer effects of GLE and more specifically of the major molecule found in GLA, annonacin. We tested and reported herein for the first time the in vivo toxicity of the GLE in mice showing that GLE can be administered safely to animals at doses up to 25 mg/kg/injection and an overall dose of about 400 mg/kg using almost daily administrations of this dose. We further tested the in vivo efficacy of GLE against human-to-mice pancreatic xenografts. Pancreatic cancer is one of the most lethal types of cancer today, and the development of novel or more efficacious approaches is an unmet medical need²⁴. Although at this dose we could not see a clear beneficial effect of GLE against xenografted tumors, there was a trend toward a delay in tumor growth. However, the total dose is much lower than the limit of the 1100 mg/kg total dose that is considered the upper limit for all clinically useful antitumor agents²⁵. Moreover, it would be of interest to test annonacin instead of the extract as this natural compound is considered the most important ingredient in terms of activity of GLE.

In regard specifically to annonacin, our in silico studies have identified this compound for the first time, as a possible strong inhibitor for both NKA and SERCA pumps. We validated our in silico findings and proved that *Graviola* is able to inhibit both NKA and SERCA activity. It has been reported that annonacins are also potent inhibitors of the NADH-ubiquinone reductase (complex I) activity of mammalian mitochondria²⁰. Thapsigargin, a known SERCA inhibitor, disrupts Ca²⁺ homeostasis, and causes cell death in cancer cells, supporting further evidence that inhibiting SERCA activity promotes cell death. Expression of different SERCA isoforms has been reported in various cancers, and our



bioprofiling studies show a strong correlation between high SERCA isoform expression and reduced cancer patient survival. Moreover, our in vivo xenograft

pancreatic model corroborates and suggests that GLE also reduces the growth rate of cancer which suggests that the active agent annonacin is a strong and promising

candidate against cancer by acting partly on reducing SERCA activity.

Ouabain, an NKA inhibitor, has previously been used for the treatment of atrial fibrillation and heart failure²². Its potential anticancer effect has also attracted great interest and it was recently shown to induce cell death in renal cancer cells. In the same study, the expression of NKA $\alpha 3$ but not the $\alpha 1$ isoform was associated with ouabain sensitivity, suggesting that isoform specificity and activity may be associated with cellular proliferation and cancer propagation²². Such study also substantiates our bioprofiling analysis showing a strong correlation between high NKA isoform expression and reduced human kidney cancer survival. Taken together, these results suggest that GLE annonacin acts via a novel signaling pathway involving both NKA and SERCA to sensitize cell death in cancer cells without affecting normal cells that may also be dependent on the expression and specificity of NKA and SERCA isoforms in cancer.

Computational analysis and docking data corroborated the similarity of annonacins with the CSs by showing a similar binding mode in the high-affinity CS-binding site, which is constituted by the transmembrane helices $\alpha M1-6$ of the catalytic α -subunit forming the extracellular ion exchange pathway^{26,27}. The lactone of CSs is one of the most important features of these compounds, which is also present in muricins.

Moreover, our in vitro data additionally show that the cell death-inducing effects of GLE annonacin may be partly mediated via an apoptotic pathway, as indicated by the increased expression of both active caspase-9 and caspase-3. The inhibition of the SERCA pump by Graviola may provoke mitochondrial activation and induce the generation of mitochondrial ROS and trigger cytochrome C caspase-9 and caspase-3 intrinsic pathways. However, we cannot rule out other cell death pathways that may be mediated by GLE annonacin such as necroptosis and autophagy-induced cell death. The NKA inhibitor, ouabain, has been shown to induce apoptosis and autophagy in Burkitt lymphoma and lung cancer cells²⁸. Similarly, SERCA inhibitors have also been reported to induce both apoptosis and autophagic cell death²⁹. Despite the differences in cell death pathways, it has been suggested that apoptosis, necroptosis, and autophagy may be intimately connected and modulated by similar regulators. Further work is required to determine whether GLE annonacin can possibly act by mediating multiple cell death pathways^{30,31}. Our study has highlighted and identified a novel pathway mediated by GLE annonacin as an inhibitor of both NKA and SERCA pumps. We propose that GLE annonacin could be targeting NKA and SERCA activity in cancer sensitizing them to cell death and therefore be a novel promising approach toward treating cancer³¹.

Materials and methods

Cell culture and reagents

MCF10-A and MCF12F cells were obtained from Barbara Ann Karmanos Cancer Institute (Detroit, MI) and were maintained in DMEM-F/12 medium containing 5% heat-inactivated horse serum, 10 $\mu\text{g}/\text{ml}$ insulin, 20 ng/ml EGF, 0.1 ng/ml cholera enterotoxin, and 0.5 $\mu\text{g}/\text{ml}$ hydrocortisone. MCF-7, PC-3, HeLa, and H1299 were cultured as NCI-PBCF-HTB22 (ATCC[®] HTB-22).

MIA PaCa-2 (ATCC[®] CRL-1420[™]) human pancreatic cancer cell line (carcinoma derived from tumor tissue of the pancreas obtained from a 65-year-old Caucasian male), purchased by ATCC (ATCC-LGC, Germany), was cultured in RPMI 1640 medium (Gibco, Grand Island, NY, USA) supplemented with 100 U/ml penicillin + 100 $\mu\text{g}/\text{ml}$ streptomycin (Gibco, Grand Island, NY, USA), 2 mM L-glutamine (Gibco, Grand Island, NY, USA), and 5% fetal bovine serum (Lonza, Verviers, Belgium), at 37 °C in a humidified atmosphere containing 5% CO₂.

In silico

Chemographic mapping with ChemGPS-NP and CheS-Mapper

In order to visualize the chemical space of the compounds of interest in 3D, and to gather information on its mechanism of action, a PCA with ChemGPS-NP³² (<http://chemgps.bmc.uu.se>) was carried out using a database of two²⁸ cancer chemotherapeutics reported in De Ford et al.³³. Subsequent cluster analysis was performed with CheS-Mapper³⁴ (<http://ches-mapper.org/>). The compounds were submitted in SMILES format and compared against the database. ChemGPS-NP comprises 35 molecular descriptors that are subdivided into eight principal components (PC) with physicochemical properties considered. Data were analyzed as previously described³³. The SMILES and PC values for the compounds tested are shown in Table 1.

Tanimoto coefficient similarity search with Knime[®]

A data pipeline was constructed in Knime[®] (Zurich, Switzerland) to compare the Tanimoto coefficient of the compounds to the database of chemotherapeutic compounds from the database. The obtained results were subsequently analyzed to obtain further information on the mechanism of action.

Docking calculations with GOLD 5.2

The crystal structures of Na⁺,K⁺-ATPase (NKA) in the E2P conformation (a high-affinity complex with ouabain; PDB ID: 4HYT)^{35,36}, in the E2·2K⁺·Pi (a low-affinity complex with ouabain; PDB ID: 3A3Y)¹⁶ were downloaded from the protein data bank^{37,38} and subjected to docking studies using GOLD 5.2 software (CCDC, Cambridge, UK). Three independent docking experiments were performed using the default docking

settings with a total of 30 genetic algorithm (GA) runs per compound for each individual experiment. The docking was allowed to terminate when the top three solutions were within the 1.5 Å root-mean-square deviation (RMSD). The active site radius was set at a distance of 15 Å from Phe783 in both NKA crystals. Intermolecular interactions were described using Discovery Studio 4.0 (Accelrys Inc., San Diego, CA, USA).

Bioprofiling

This method was used to analyze biological data of recently developed analytical tools for genomics, proteomics, and metabolomics³⁹.

Na⁺ and K⁺-ATPase activity

NKA membranes were purified from pig kidney outer medulla, as previously described⁴⁰. The ATPase activity assay was carried out at 37 °C in a medium consisting of 130 mM NaCl, 20 mM KCl, 4 mM MgCl₂, 3 mM ATP, and 20 mM histidine (pH 7.4)⁴¹. The enzyme was incubated with varying concentrations of the compounds for 30 min at 37 °C prior to the addition of ATP. Specific Na and K-ATPase activity was calculated as the difference in Pi release in the absence and presence of 1 mM ouabain⁴⁰. The data on residual Na and K-ATPase activity are presented as a function of inhibitor concentration.

In situ measurements of SERCA activity

Cells were transiently transfected with the ER-targeted genetically encoded FRET Ca²⁺ sensor vYEC4-ER and measured in single cells as previously described^{42,43}. Experiments with the ER were completely emptied by preincubation with 15 μM BHQ and 10 μM histamine in the nominal absence of extracellular Ca²⁺. After reaching a stable minimum, the agonists and BHQ were washed, and the compound to be tested was added 1 min prior to re-addition of extracellular Ca²⁺. SERCA activity is reflected by the kinetics of ER refilling compared with controls.

Extraction

Two “Graviola” capsules provided from “Advance Physician Formulas” (500 mg per tablet) were diluted in absolute ethanol, followed by 24 h of stirring in room temperature incubation. The extract was centrifuged at 5000 rpm for 5 min, collected, filtered, and evaporated using a rotary evaporator at 45 °C. The concentrated sample was resuspended in 3 ml of absolute ethanol and filtered through a sterile micropore (2.2 μm). Finally, the pure extract re-evaporated by nitrogen gas and reweighted to quantitate the extract (124 mg; yield = 24.8%).

Molecular isolation and characterization

Thin-layer chromatography

A standard method was used according to Patrikios et al. The developing solvent system used was HPLC-grade ethanol:water (80:20 ml/ml). The developed chromatogram was observed under iodine vapor⁴⁴.

Liquid chromatography–mass spectrometry analysis

An aliquot of the dried extract was resuspended in 20% acetonitrile, 0.1% trifluoroacetic acid solution, and purified by solid-phase extraction using an Oasis 10-mg HLB cartridge. The eluted sample was lyophilized using a centrifugal vacuum evaporator and redissolved in 35% acetonitrile and 0.1% formic acid solution prior to LC–MS analysis. Chromatographic analysis of the sample was performed on an Acquity I-Class UPLC system using an Acquity UPLC HSS T3 (2.1 × 150 mm, 1.8 mm) analytical column. Column temperature was set to 45 °C and the injection volume was 2 μL. A gradient elution with a total run time of 40 min was performed at a flow rate of 0.4 ml/min. Briefly, initial conditions of 35% of mobile phase A (0.1% formic acid in water) were kept for 5 min, followed by a linear gradient from 65 to 85% of mobile phase B (0.1% formic acid in acetonitrile) in 20 min, column wash with 9% mobile phase B for 7 min, and column equilibration to initial conditions for 8 min. Full-scan MS data from 400 to 800 *m/z* were collected on a Waters Xevo TQD MS instrument in a positive ion mode.

ESI-QTOF-MS analysis

A single LC fraction (11.70–12.20 min) was collected, evaporated to dryness, redissolved in 50% methanol and 0.1% formic acid, and subjected directly to high-resolution MS analysis. The analysis was performed on a Synapt G2-Si HDMS instrument (Waters, UK) equipped with the standard z-spray electrospray ionization (ESI) source. The spectrum was acquired in an ion-positive mode. Instrument control and data processing were performed using the Waters MassLynx™ 4.1 data system. The sample was infused using a syringe pump (Harvard Syringe Pump, model 55–2222, Holliston, MA, USA) and a 100-μL Hamilton syringe (Bonaduz, Switzerland), at a flow rate of 5 μL/min.

LIVE/DEAD® Viability/Cytotoxicity Kit “for mammalian cells”

The viability assay was performed according to Molecular Probes Invitrogen Detection Technologies. Revised: 21 December 2005.

Wound-healing assay

The wound-healing assay was performed according to Jonkman, James E. N. et al⁴⁵.

Western blotting analysis

After treatment, the cells were washed twice with PBS and scraped with lysis buffer (4% sodium dodecyl sulfate, 20% glycerin, 20 mM Tris-HCl, 1 mM PMSF, 1 mM NaF, and 200 μ M Na₃VO₄). Then, they were loaded onto each lane of a 12 or 15% SDS-polyacrylamide gel for electrophoresis and transferred onto nitrocellulose membranes. Primary antibodies (Cell Signaling, Danvers, MA, USA) were incubated overnight at 1/1000 dilution. Horseradish peroxidase-conjugated secondary antibodies (DAKO, Ely, UK) were used at 1/5000 dilution. In all cases, membranes were blocked with 5% skim milk in TBST (10 mM Tris-HCl, 0.1 M NaCl₂, and 0.5% Tween 20, pH 8.0) for 2 h at room temperature. After blocking, membranes were incubated for 2 h with an anti-human primary antibody at room temperature followed by overnight incubation at 4 °C. After washing with TBST three times, the membranes were incubated with the corresponding secondary antibody for 1 h at room temperature. The protein bands were detected using the Western Luminescent Detection Kit. Finally, the Western blot images were analyzed using the ChemiDoc XRS system with actin and tubulin used as the protein control.

Caspase-3/7 activity assay

The assay was performed according to the manufacturer's protocol. CellEvent™ Caspase-3/7 Green Detection Reagent was purchased.

MTT Cell Growth Assay Kit

Cell viability tests were performed according to the manufacturer's protocol Cell Proliferation Kit J (MTT).

Cell viability was measured as a percentage of cell survival in drug-treated cells relative to untreated cells. The results are reported as mean from three different experiments performed at least in triplicate, $p < 0.05$.

In vivo toxicity study

For the in vivo toxicity study, NOD.CB17-Prkdc^{scid}/J mice bred in our breeding facility (EL-42BIO/br-01, Panepistimiopolis, Larissa, Greece) were used. The mouse colony was maintained in a pathogen-free environment in type 1 cages. Female mice, 6–8-weeks old, were used in the studies described here. During the experiments, all animals were kept under specific pathogen-free conditions at the animal facility of our department (EL42-BIO/exp-03) and allowed ad libitum feed and water. Acute toxicity determination to find the MTD for the animals was performed following the guidelines of the NCI as described elsewhere. Extracts were administered in a 10% DMSO/5% Cremophor ELP (BASE, Ludwigshafen, Germany)/PBS carrier. An animal that received only the carrier was used as control to exclude any side effects due to the carrier. The drug was administered intraperitoneally in mice at a

volume of 20 μ L/1 g of weight, and the volume was adjusted for the weight of each individual mouse. For the needs of this experiment, the parameters observed and recorded were survival, weight loss, and behavioral changes for a period of 2 weeks, and two independent series of experiments were performed.

Experimentation and handling of animals were performed in accordance to the Greek laws (PD 56/2003 and Circular 2215/117550/2013) and to the guidelines of the European Union (2013/63/EU).

To generate xenografts, exponentially growing cultures of MIA PaCa-2 human pancreatic cancer cells were subcutaneously injected at the axilla region of 8–10-week-old female NOD.CB17Prkdc^{scid}/J mice from our animal facility (1×10^6 cells/injection, one injection per mouse). When the tumors reached a size of about 200 mm³ (advanced-stage model), the mice were arbitrarily divided into three groups and each group consisted of eight mice ($n = 8$ /group). Subsequently, mice were treated intraperitoneally once per day for 3 weeks (15 administrations) either with vehicle (10% DMSO and 5% Cremophore in 0.9% NaCl) or paraviola extract (25 mg/kg). One group received no treatment and served as the control group. Mean tumor volume and standard deviation (SD) for all groups were calculated, and growth curves were plotted as a function of time. In order to study the in vivo effect of the extract, mean tumor volume and SD for all groups were calculated, and growth curves were plotted as a function of time. Tumor volume was calculated according to the formula $[(a \times b^2)/2]$, where a = length and b = width of the tumor as measured with a vernier's caliper (measurements were performed twice a week). When tumor volume reached a size of approximately 10% of the mouse weight (2000–2200 mm³), mice were euthanized. Mice were also weighed to monitor toxicity twice a week.

Statistical analysis

Statistical analysis was performed using ANOVA or Student's t -test and the GraphPad Prism version 6 software package (GraphPad Software, Inc., La Jolla, USA). A $p < 0.05$ was considered as statistically significant.

Acknowledgements

C.D.F. is grateful for a DAAD doctoral fellowship. This research was partly supported by the Excellence Initiative of the German Research Foundation (GSC-4, Spemann Graduate School).

Authors' contributions

Y.A., P.I., and S.A. drafted the manuscript. J.E., D.K., D.F.C., W.G., and S.K. critically revised the manuscript. All authors have read and approved the manuscript for publication.

Author details

¹School of Medicine, European University Cyprus, Nicosia, Cyprus. ²School of Medicine, National and Kapodestrian University of Athens, Athens, Greece.

³Department of Pharmacology, School of Health Sciences, University of Thessaly, Volos, Greece. ⁴Department of Pharmaceutical Biology and Biotechnology, Spemann Graduate School of Biology and Medicine (SGBM), Albert Ludwigs University Freiburg, Freiburg, Germany. ⁵Department of Biomedicine-Physiology and Biophysics, Aarhus University, Aarhus, Denmark. ⁶Gottfried Schatz Research Center, Molecular Biology & Biochemistry, Medical University of Graz, Graz, Austria. ⁷Department of EM/Molecular Pathology, Institute of Neurology and Genetics, Nicosia, Cyprus

Conflict of interest

The authors declare that they have no conflict of interest.

Publisher's note

Springer Nature remains neutral with regard to jurisdictional claims in published maps and institutional affiliations.

Received: 2 April 2018 Revised: 7 May 2018 Accepted: 10 May 2018

Published online: 09 July 2018

References

- Mishra, S., Ahmad, S., Kumar, N. & Sharma, B. K. *Annona muricata* (the cancer killer): a review. *Glob. J. Pharm. Res.* **2**, 1613–1618 (2013).
- Leboeuf, M., Cavé, A., Bhaumik, P., Mukherjee, B. & Mukherjee, R. The phytochemistry of the annonaceae. *Phytochemistry* **21**, 2783–2813 (1980).
- Adeyemi, S. O. & Caxton-Martins, E. A. Morphological changes and hypoglycemic effects of *Annona muricata* Linn. (Annonaceae) leaf aqueous extract on pancreatic B-cells of streptozotocin-treated diabetic rats. *Afr. J. Biomed. Res.* **9**, 173–187 (2006).
- De Sousa, O. V., Vieira, G. D.-V., de Pinho, J. D. J. R., Yamamoto, C. H. & Alves, M. S. Antinociceptive and anti-inflammatory activities of the ethanol extract of *Annona muricata* L. leaves in animal models. *Int. J. Mol. Sci.* **11**, 2067–2078 (2010).
- Adeyemi, S. & Ojewole, J. Protective effects of *Annona muricata* Linn. (Annonaceae) leaf aqueous extract on serum lipid profiles and oxidative stress in hepatocytes of streptozotocin-treated diabetic rats. *Afr. J. Tradit. Complement. Altern. Med.* **6**, 30–41 (2009).
- Watt, J. M. & Breyer-Brodwijik, M. *The Medicinal and Poisonous Plants of Southern and Eastern Africa: Being an Account of Their Medicinal and Other Uses, Chemical Composition, Pharmacological Effects and Toxicology in Man and Animal*. (Livingstone Ltd., Edinburgh; London, 1962).
- McLaughlin, J. L. Paw paw and cancer: annonaceous acetogenins from discovery to commercial products. *J. Nat. Prod.* **51**, 1311–1321 (2008).
- María, T. et al. Graviola: a novel promising natural derived drug that inhibits tumorigenicity and metastasis of pancreatic cancer cells in vitro and in vivo through altering cell metabolism. *Cancer Lett.* **323**, 29–40 (2012).
- Dai, Y. et al. Selective growth inhibition of human breast cancer cells by Graviola fruit extract in vitro and in vivo involving downregulation of EGFR expression. *Nutr. Cancer* **5**, 795–801 (2011).
- Burris, H. A. et al. Improvements in survival and clinical benefit with gemcitabine as first-line therapy for patients with advanced pancreas cancer: a randomized trial. *J. Clin. Oncol.* **15**, 2403–2413 (1997).
- Sun, S. et al. Isolation of three new annonaceous acetogenins from Graviola (*Annona muricata*) and their anti-proliferation on human prostate cancer cells. *3-Bioorg. Med. Chem. Lett.* **26**, 4382–4385 (2016).
- Yap, J. et al. Synergistic interactions among flavonoids and acetogenins in Graviola (*Annona muricata*) leaves confer protection against prostate cancer. *Carcinogenesis* **36**, 656–665 (2015).
- Deep, G. et al. Graviola inhibits hypoxia-induced NADPH oxidase activity in prostate cancer cells reducing their proliferation and colonogenicity. *Sci. Rep.* **6**, 23135 (2016).
- Allegrand, J. et al. Structural study of acetogenins by tandem mass spectrometry under high and low collision energy. *Rapid Commun. Mass Spectrom.* **24**, 3602–3608 (2010).
- Bonneau, N., Schmitz-Afonso, I., Touboul, D., Brunelle, A. & Champy, P. Method development for quantitation of the environmental neurotoxin annonacin in Rat plasma by UPLC-MS/MS and its application to a pharmacokinetic. *J. Chromatogr. B Anal. Technol. Biomed. Life Sci.* **1004**, 46–52 (2015).
- Ogawa, H., Shinoda, T., Cornelius, F. & Toyoshima, C. Crystal structure of the sodium-potassium pump (Na⁺/K⁺-ATPase) with bound potassium and ouabain. *Proc. Natl. Acad. Sci. USA* **106**, 13742–13747 (2009).
- Pimenta, H. C., Silva, C. L. M. & Noëll, F. Ivermectin is a nonselective inhibitor of mammalian P-type ATPases. *Naunyn Schmiede. Arch. Pharmacol.* **381**, 147–152 (2010).
- Yatime, L. et al. P-type ATPases as drug targets: tools for medicine and science. *Biochim. Biophys. Acta Bioenerg.* **1787**, 207–220 (2009).
- Prassas, I. & Diamandis, E. P. Novel therapeutic applications of cardiac glycosides. *Nat. Rev. Drug Discov.* **7**, 926–935 (2008).
- Degli Esposti, M., Ghelli, A., Ratta, M., Cortes, D. & Estornell, E. Natural substances (acetogenins) from the family Annonaceae are powerful inhibitors of mitochondrial NADH dehydrogenase (complex I). *Biochem. J.* **301**, 1161–1167 (1994).
- Frieden, M., Malli, R., Samardzija, M., Demareux, N. & Gajda, W. F. Sub-plasmalemmal endoplasmic reticulum controls K_{Ca} channel activity upon stimulation with a moderate histamine concentration in a human umbilical vein endothelial cell line. *J. Physiol.* **550**, 73–81 (2002).
- Chemaly, E. R., Troncone, L. & Lebel, D. SERCA control of cell death and survival. *Cell Calcium* **69**, 46–61 (2018).
- Pongrakhananon, V., Chibbarha, P. & Chanvorachote, P. Ouabain suppresses the migratory behavior of lung cancer cells. *PLoS ONE* **8**, e68623 (2013).
- Sereti, E. et al. Patient derived xenografts (PDX) for personalized treatment of pancreatic cancer: a review. *Proteomics*, 1874–3001 (18) 30043–5 (2018).
- Corbett, T. et al. in *Anticancer Drug Development Guide: Preclinical Screening, Clinical Trials and Approval* (eds Teicher, B.A. & Andrews, P.A.) 2nd edn, 99–124 (Humana Press Inc., NJ; USA 2004).
- Qiu, L. Y., Klenderink, J. B., Swarts, H. G. P., Willems, H. G. M. & De Pont, H. H. M. Phe783, Thr797, and Asp804 in transmembrane hairpin M5-M6 of Na⁺/K⁺-ATPase play a key role in ouabain binding. *J. Biol. Chem.* **278**, 47240–47244 (2003).
- Feig, J. & Lingrel, J. B. Analysis of amino acid residues in the H5-H6 transmembrane and extracellular domains of Na₂K-ATPase alpha subunit identifies threonine 797 as a determinant of ouabain sensitivity. *Biochemistry* **33**, 4218–4224 (1994).
- Xiao, Y. et al. Ouabain targets the Na⁺/K⁺-ATPase α3 isoform to inhibit cancer cell proliferation and induce apoptosis. *Oncol. Lett.* **14**, 6678–6684 (2017).
- Wong, V. K. W. et al. Saikosaponin-d, a novel SERCA inhibitor, induces autophagic cell death in apoptosis-defective cells. *Cell Death Dis.* **4**, e720 (2013).
- Patrikios, I., Stephanou, A. & Yiallouris, A. Graviola: a systematic review on its anticancer properties. *Am. J. Cancer Prev.* **3**, 128–131 (2015).
- Yiallouris, A., Stephanou, A. & Patrikios, I. Anticancer properties of Na⁺/K⁺-ATPase: a mini review. *Asian J. Sci. Technol.* **07**, 2864–2868 (2015).
- Rosén, J. et al. ChemGPS-NP(Web): chemical space navigation online. *J. Comput. Aided Mol. Des.* **23**, 253–259 (2009).
- De Ford, C. et al. Discovery of tricyclic clerodane diterpenes as sarco/endoplasmic reticulum Ca²⁺-ATPase inhibitors and structure–activity relationships. *J. Nat. Prod.* **78**, 1262–1270 (2015).
- Gütlein, M., Karwath, A. & Kramer, S. CheS-Mapper. Chemical space mapping and visualization in 3D. *J. Chemin.* **4**, 1–16 (2012).
- Laursen, M., Gregersen, J. L., Yatime, L., Nissen, P. & Fedosova, N. U. Structures and characterization of digoxin- and bufalin-bound Na⁺/K⁺-ATPase compared with the ouabain-bound complex. *Proc. Natl. Acad. Sci. USA* **112**, 1755–1760 (2015).
- Obara, K. et al. Structural role of countertransport revealed in Ca²⁺ pump crystal structure in the absence of Ca²⁺. *Proc. Natl. Acad. Sci. USA* **102**, 14489–14496 (2005).
- Bertha, H. et al. The protein data bank. *Nucleic Acids Res.* **28**, 235–242 (2000).
- Amelio, I. et al. SynTarget: an online tool to test the synergetic effect of genes on survival outcome in cancer. *Cell Death Differ.* **23**, 912 (2016).
- Esmann, M. ATPase and phosphatase activity of Na⁺/K⁺-ATPase: molar and specific activity, protein determination. *Methods Enzymol.* **156**, 105–115 (1988).
- Klodos, I., Esmann, M. & Post, R. L. Large-scale preparation of sodium-potassium ATPase from kidney outer medulla. *Kidney Int.* **62**, 2097–2100 (2002).
- Malli, R. et al. Sustained Ca²⁺ transfer across mitochondria is essential for mitochondrial Ca²⁺ buffering, store-operated Ca²⁺ entry, and Ca²⁺ store refilling. *J. Biol. Chem.* **278**, 44769–44779 (2003).

42. Zoratti, C., Kipmen-Korgun, D., Osibow, K., Malli, R. & Graier, W. F. Anandamide initiates Ca²⁺ signaling via CB2 receptor linked to phospholipase C in calf pulmonary endothelial cells. *Br. J. Pharmacol.* **140**, 1351–1362 (2003).
43. Patrikios, I. Lipid extracts isolated from heat processed food show a strong agglutinating activity against human red blood cells. *Food Res. Int.* **35**, 535–540 (2002).
44. Jonkman, J. et al. An introduction to the wound healing assay using live-cell microscopy. *Cell Adh. Migr.* **8**, 440–451 (2014).
45. latrou, H. et al. From polypeptide containing triblock Co- and terpolymers for drug delivery against pancreatic cancer: asymmetry of the external hydrophilic blocks. *Macromol. Biosci.* **14**, 1222–1238 (2014).

RETRACTED ARTICLE